Ann. Geophys., 26, 3269–3277, 2008
www.ann-geophys.net/26/3269/2008/

Annales Geophysicae

Survey of ELF-VLF plasma waves in outer radiation belt observed by Cluster STAFF-SA experiment

D. Pokhotelov[1], **F. Lefeuvre**[2], **R. B. Horne**[3], **and N. Cornilleau-Wehrlin**[4,5]

[1]Department of Electronic & Electrical Engineering, University of Bath, BA2 7AY, Bath, UK
[2]LPCE, 3A Avenue de la Recherche Scientifique, 45071, Orléans, France
[3]British Antarctic Survey, Natural Environment Research Council, CB3 0ET, Cambridge, UK
[4]CETP/IPSL, 10–12 Avenue de l'Europe, 78140, Vélizy, France
[5]Station de Radioastronomie de Nançay, Observatoire de Paris/CNRS, 18330, Nançay, France

Received: 31 October 2007 – Revised: 16 April 2008 – Accepted: 12 August 2008 – Published: 21 October 2008

Abstract. Various types of plasma waves have profound effects on acceleration and scattering of radiation belt particles. For the purposes of radiation belt modeling it is necessary to know statistical distributions of plasma wave parameters. This paper analyzes four years of plasma wave observations in the Earth's outer radiation belt obtained by the STAFF-SA experiment on board Cluster spacecraft. Statistical distributions of spectral density of different plasma waves observed in ELF-VLF range (chorus, plasmaspheric hiss, magnetosonic waves) are presented as a function of magnetospheric coordinates and geomagnetic activity indices. Comparison with other spacecraft studies supports some earlier conclusions about the distribution of chorus and hiss waves and helps to remove the long-term controversy regarding the distribution of equatorial magnetosonic waves. This study represents a step towards the development of multi-spacecraft database of plasma wave activity in radiation belts.

Keywords. Magnetospheric physics (Energetic particles, precipitating; Plasma waves and instabilities)

1 Introduction

Earth's radiation belt, where energetic plasma particles are trapped by the DC magnetic field, consists of two major parts known as inner and outer radiation belts. The inner radiation belt represents a relatively stable population of trapped protons and electrons with a density peak at the distance of ∼1.8 Earth radii (R_E). In contrast to the inner belt, the outer radiation belt has a highly variable particle population in which mostly electrons are trapped though a substantial component of trapped high-energy (few 100 keV) ions is also present (e.g. Davis and Williamson, 1963). For electron energies above 1 MeV the outer radiation belt peaks at a distance of $\sim 4\,R_E$. The dynamics of the outer radiation belt are governed by radial transport, acceleration and loss due to wave-particle interactions (e.g. Lyons and Thorne, 1973). Various types of electromagnetic waves that are present in the outer radiation belt can contribute into acceleration and/or pitch angle scattering of particles into the loss cone.

Development of physical models for particle diffusion in the outer radiation belt such as Salammbô model (Bourdarie et al., 1996) requires a knowledge of diffusion coefficients related to the wave-particle interaction processes. In order to estimate the pitch angle diffusion coefficients it is necessary to know distributions of the intensity of various plasma waves within outer radiation belts. A few efforts have been made recently to create statistical databases of wave properties using Dynamic Explorer 1 (DE-1) (André et al., 2002; Green et al., 2005) and CRRES (Meredith et al., 2001, 2004) spacecraft. However, all existing databases use the data from a single spacecraft and thus have limited spatial coverage. For instance, low-inclination CRRES orbit does not allow us to analyze the regions outside ±30° MLat, while high-inclination DE-1 orbit does not provide complete MLT coverage. The ideal statistical database for radiation belt modeling would thus have to combine the data from few satellite missions with different orbit types. High-inclination Cluster orbit allows to study wave distributions at high latitudes as well as to look at the important region of chorus generation

Correspondence to: D. Pokhotelov
(d.pokhotelov@bath.ac.uk)

Published by Copernicus Publications on behalf of the European Geosciences Union.

presumably located near magnetic equator at the edge of plasmasphere (e.g. Parrot et al., 2003).

2 Types of electromagnetic waves observed in radiation belts

Various types of plasma waves in the ULF-VLF frequency range can interact with radiation belt particles causing pitch angle diffusion and/or acceleration of trapped particles. A summary of the wave types that can contribute to acceleration and loss was given by Horne and Thorne (1998). The current study focuses on plasma waves occurring in the ELF and VLF frequency ranges between proton cyclotron frequency f_{cH} and electron cyclotron frequency f_{ce}. Plasma waves important for the radiation belt dynamics in this frequency range include chorus, plasmaspheric hiss and equatorial magnetosonic waves.

Chorus emissions are coherent right-hand polarized whistler mode waves observed near and outside the plasmapause, characterized by discrete structure of the dynamic spectrum (e.g. Russell et al., 1972; Storey et al., 1991; Sazhin and Hayakawa, 1992). Chorus is observed in a frequency band running from 0.1 to 0.8 f_{ce} and often structured in two distinct bands: one above and one below 0.5 f_{ce} (Tsurutani and Smith, 1977). It has been suggested that the chorus emissions play an important role in the rapid electron acceleration during magnetic storms from energies of ∼100 keV to above 1 MeV (Horne and Thorne, 1998; Summers et al., 1998). Experimental evidences of storm-time chorus acceleration have been recently presented by Horne et al. (2005).

Plasmaspheric hiss represent broad-band incoherent whistler mode waves mainly confined by the plasmasphere and observed in the frequency range from few hundreds of hertz to ∼2 kHz (e.g. Taylor and Gurnett, 1968; Thorne et al., 1973; Cornilleau-Wehrlin et al., 1978). Hiss is believed to be generated inside the plasmasphere in contrast to the chorus waves generated outside. Statistical parameters of hiss emissions including the dominant direction of wave vectors have been analyzed by Parrot and Lefeuvre (1986) and Santolík and Parrot (2000). Plasmaspheric hiss is believed to be among the dominant mechanisms of pitch angle scattering for radiation belt electrons (Abel and Thorne, 1998). Sonwalkar and Inan (1989) suggested that the plasmaspheric hiss emissions can be triggered by lightning-induced whistlers. Pitch-angle scattering of energetic electrons by plasmaspheric hiss largely accounts for the formation of the slot region that separates the inner and outer radiation belts (Lyons and Thorne, 1973; Abel and Thorne, 1998; Meredith et al., 2006).

Equatorial magnetosonic waves (often referred as "equatorial electromagnetic noise") have been first reported by Russell et al. (1969) and studied in detail by Perraut et al. (1982), Kasahara et al. (1994) and Santolík et al. (2004). The magnetosonic waves are linearly polarized compressional mode waves usually observed in multiple frequency bands situated near harmonics of local proton gyrofrequency with a cutoff at lower-hybrid frequency $f_{lh} = (f_{ce} f_{cH})^{1/2}$. These waves are known to propagate nearly perpendicular to the background magnetic field and appear very close to the magnetic equator. Russell et al. (1970) first suggested that the equatorial magnetosonic emissions may interact with radiation belt particles and recent numerical simulations by Horne et al. (2007) outlined the importance of magnetosonic waves for the relativistic electron acceleration.

3 Cluster STAFF-SA experiment and data selection

Cluster is a constellation of four identical highly elliptical orbit spacecraft launched in July–August 2000. Cluster orbit perigee and apogee are, respectively, 20 000 km and 120 000 km with an orbit inclination of 91° and a period of 3426 min. Cluster spacecraft cross the Earth's magnetic equator near L=4 covering the large portion of outer radiation belts.

The STAFF-SA (Spatio-Temporal Analysis of Field Fluctuations – Spectrum Analyzer) experiment (Cornilleau-Wehrlin et al., 1997) includes on-board spectrum analyzer with 27 frequency channels logarithmically spaced between 8.8 Hz and 3.56 kHz. The on-board spectrum analyzer calculates the complete spectral matrix (real and imaginary part) of the three magnetic components measured by the STAFF search coil magnetometer and the two electric field components from the EFW experiment (Gustafsson et al., 2001) with a time resolution that is generally 1 s. Out of the spectral matrix coefficient for this study we will use the magnetic field spectral density. The sensitivity of STAFF search coil magnetometers is 4×10^{-4} nT/Hz$^{1/2}$ and 1×10^{-5} nT/Hz$^{1/2}$, respectively, at 10 Hz and 1 kHz frequency. In this study care has been taken to exclude the values of spectral density falling below the magnetometer sensitivity curve presented by Cornilleau-Wehrlin et al. (2003).

Current survey includes STAFF-SA data from the first Cluster spacecraft (Rumba) for the period from March 2001 to February 2005. The remaining STAFF-SA data is available at the ESA Cluster Active Archive and can be added to the database in the future. Magnetic coordinates (MLT, MLat an L-shell) of the spacecraft and the local values of f_{ce} have been obtained from the Cluster Predicted Magnetic Position catalogues (Hapgood et al., 1997). In order to study waves that may be relevant to the outer radiation belt we only considered those intervals when spacecraft was situated between ±45° MLat and inside the magnetic shell L=9.

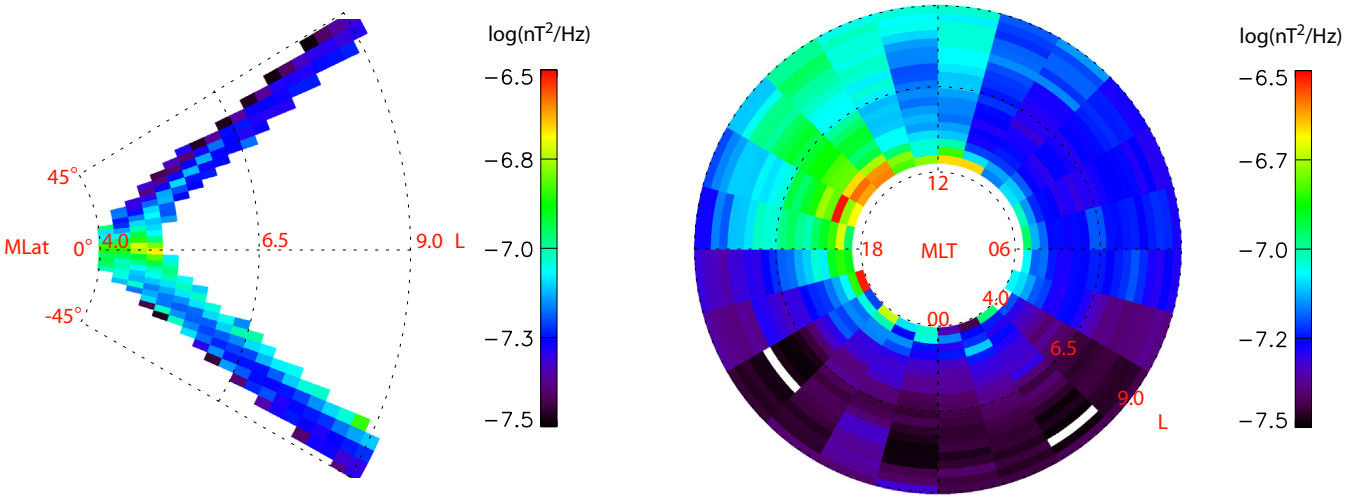

Fig. 1. Distribution of the spectral density in the frequency range $0.0005 \leq f/f_{ce} < 0.02$ dominated by magnetosonic waves.

4 Distributions of spectral density

4.1 Construction of the database

For the purposes of computing the pitch angle diffusion coefficients (e.g. Glauert and Horne, 2005) it is necessary to express the statistical distributions of wave spectral density as a function of magnetic coordinates MLT, MLat and L-shell. In this study the statistical distributions of spectral density have been obtained by logarithmic averaging of all values of spectral density measured within a particular sector in MLT-L-MLat coordinates.

The dimensions of database sectors are 1 h in MLT, 0.25 L in L-shell values and 2.5° in MLat. The distributions in MLT-L coordinates (magnetic equator plane) are computed by logarithmic averaging over all MLat sectors, and the distributions in MLat-L coordinates (magnetic meridian plane) are obtained by averaging over all MLT sectors.

Since the value of local cyclotron frequency is the meaningful parameter for propagation and generation of various plasma waves, it is useful to construct the distributions of spectral density in terms of the normalized frequency f/f_{ce}. Normalized frequency bands used in this study are shown in Table 1. Taking into account the properties of plasma waves described above we assume that the frequency band $0.0005 \leq f/f_{ce} < 0.02$ between local f_{cH} and local f_{lh} is dominated by equatorial magnetosonic waves, the frequency band $0.02 \leq f/f_{ce} < 0.1$ is dominated by plasmaspheric hiss, the frequency band $0.1 \leq f/f_{ce} < 0.5$ is dominated by lower-band chorus, and the band $0.5 \leq f/f_{ce} < 1$ covers upper-band chorus waves. This study is limited to the frequency ranges above local proton gyrofrequency f_{cH} due to the bandwidth of Cluster STAFF-SA experiment. For the study of lower frequency waves one should use the STAFF experiment wave form data that in the normal mode of operation covers 0.3–10 Hz frequency range.

Table 1. Frequency ranges used in the database.

Frequency range	Wave type
$0.0005 \leq f/f_{ce} < 0.02$	Magnetosonic waves
$0.02 \leq f/f_{ce} < 0.1$	Plasmaspheric hiss
$0.1 \leq f/f_{ce} < 0.5$	Lower-band chorus
$0.5 \leq f/f_{ce} < 1$	Upper-band chorus

4.2 Magnetosonic waves

Statistical distribution of spectral density in the frequency range $0.0005 \leq f/f_{ce} < 0.02$ dominated by equatorial magnetosonic waves is shown in Fig. 1. L-MLT and L-MLat distributions in Fig. 1 clearly demonstrate that the spectral density of magnetosonic waves is concentrated within 5–7° MLat from the magnetic equator which is consistent with earlier findings (e.g. André et al., 2002; Santolík et al., 2004).

It has to be mentioned that the MLT distribution of equatorial magnetosonic emissions became a subject of long-term controversy. Russell et al. (1969) using OGO-3 observation near the equatorial plasmapause and Kasahara et al. (1994) using Akebono data from deep inside the plasmasphere reported no visible dependance on local time, while Perraut et al. (1982) analyzing GEOS-2 geostationary orbit data found maximum intensity of the magnetosonic emissions in the post-noon MLT sector. Figure 1 clearly shows the maximum of wave spectral density in 12:00–18:00 MLT sector thus confirming the conclusions of Perraut et al. (1982).

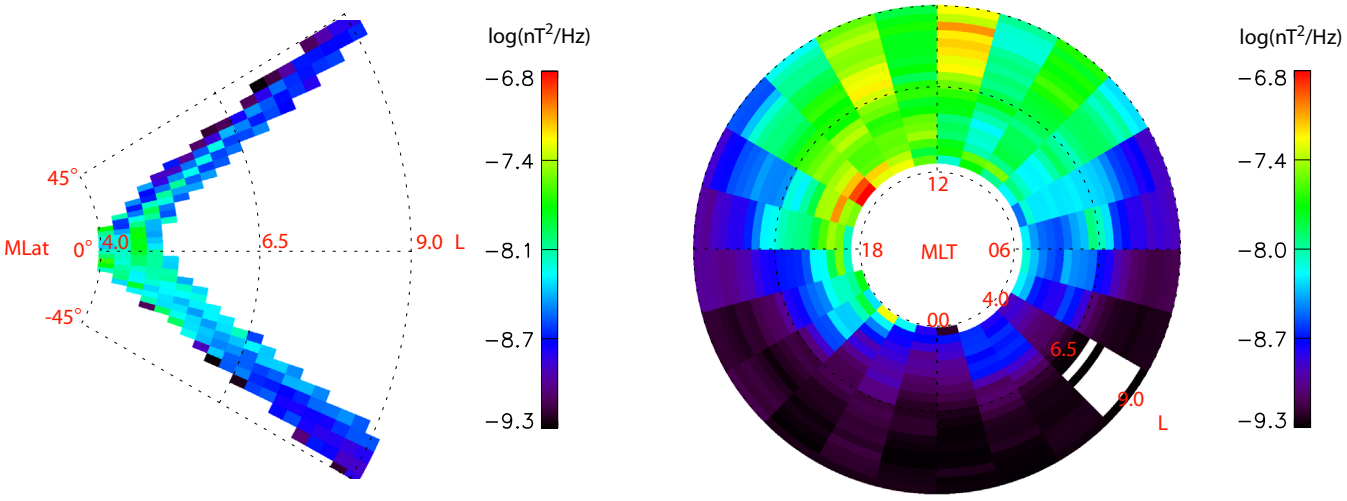

Fig. 2. Distribution of the spectral density in the frequency range $0.02 \leq f/f_{ce} < 0.1$ dominated by plasmaspheric hiss.

One has to remember that the distributions of spectral density given in this paper represent statistical values averaged over time, spatial sector and frequency band. Consequently, the statistically averaged values may appear very low comparing to the peak magnitudes of specific plasma wave events reported elsewhere. This is particularly noticeable in the case of equatorial magnetosonic emissions due to the facts that: (1) the intensity of magnetosonic waves changes dramatically with frequency with peak magnitudes typically near 10 f_{cH}; and (2) the intensity of magnetosonic waves falls sharply with latitude. For example, peak magnitudes of the magnetosonic waves observed by Cluster during specific events can reach $\sim 10^{-2}$ nT^2/Hz (see Fig. 1 in Horne et al., 2007) while statistical averages of the spectral density presented in this paper are lower by a few orders of magnitude.

4.3 Plasmaspheric hiss

Earlier studies suggested that plasmaspheric hiss appear at all frequencies from 100 Hz up to 2–3 kHz with spectral intensity peaking near a few hundred Hz (Thorne et al., 1973; Cornilleau-Wehrlin et al., 1978; Meredith et al., 2004). In this paper we assume plasmaspheric hiss to be dominant in the frequency range above the local f_{lh} (0.02 f_{ce}) and below 0.1 f_{ce}. These restrictions on hiss frequency band are imposed to avoid contributions of plasmaspheric hiss into spectral bands of magnetosonic and lower-band chorus emissions. As been already noted the hiss frequency band is generally not related to the local gyrofrequency (e.g. Meredith et al., 2004) and while the above definition of hiss band is valid near the equator at L=4.5 where Cluster crosses the equator, at higher latitudes along Cluster orbit hiss emissions can potentially contribute into the spectral bands of other emissions. Magnetosonic waves are confined to the equatorial region and thus potential contribution of hiss into the magnetosonic band at high latitudes can be easily identified. Contribution of hiss into lower-band chorus spectra is likely to be small in most regions since the intensity of hiss falls rapidly above 1 kHz (Meredith et al., 2004). More sensible discrimination between hiss, chorus and magnetosonic emissions can be achieved by analyzing coherency of measured magnetic components (e.g. Cornilleau-Wehrlin et al., 1978; Lefeuvre and Parrot, 1979) but such analysis is beyond the scope of this paper.

Distribution of spectral density in the frequency range $0.02 \leq f/f_{ce} < 0.1$ is shown in Fig. 2. Hiss emissions appear in all MLT sectors from 06:00 to 18:00 MLT inside $L \sim 6$ with maximum magnitudes in the post-noon sector. Original paper by Thorne et al. (1973) suggested that plasmaspheric hiss can be found at all MLT, and few recent studies (e.g. André et al., 2002; Meredith et al., 2004; Green et al., 2005) have demonstrated that these waves occur primarily on the day side with maximum intensities in the post-noon MLT sector which is consistent with the distributions presented here. Relatively high spectral densities that are seen in Fig. 2 in the noon sector at high L-shells ($L > 6.5$) appear far outside the plasmapause and most likely are caused by lower-band chorus contributing into the hiss band.

4.4 Lower- and upper-band chorus

Left- and right-hand panels in Fig. 3 show the distributions of spectral density in MLat-L and MLT-L coordinates, respectively, for the frequency range $0.1 \leq f/f_{ce} < 0.5$ which is dominated by lower-band chorus.

The distributions in Fig. 3 show chorus waves appearing in all sectors from 05:00 to 18:00 MLT with a maximum intensity in post-noon sector. Unlike equatorial magnetosonic waves and hiss, chorus intensity maximizes near 10° MLat

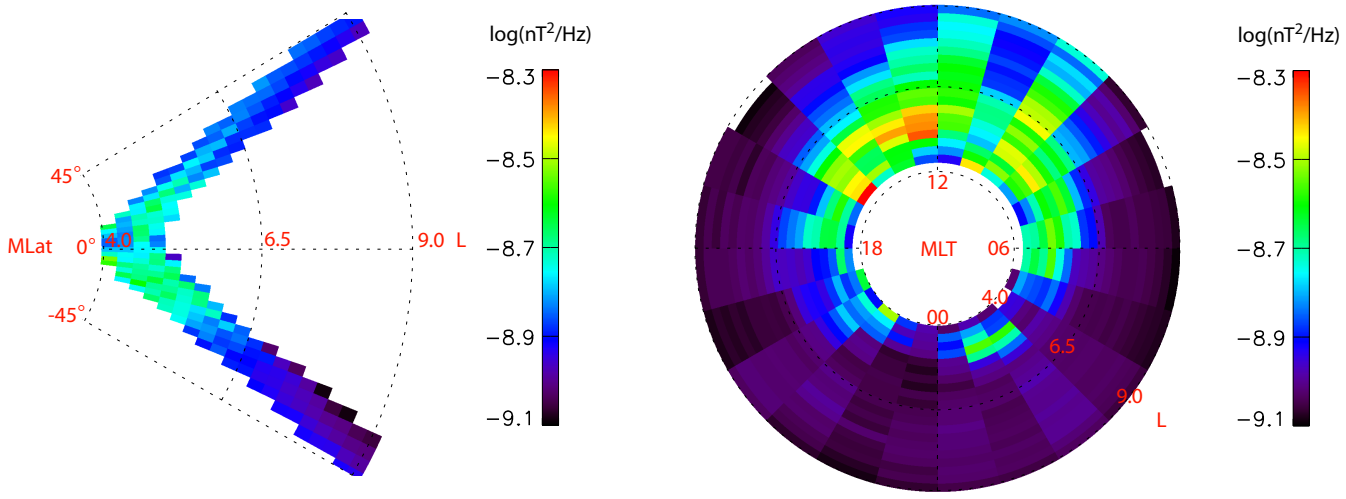

Fig. 3. Distribution of the spectral density in the frequency range $0.1 \leq f/f_{ce} < 0.5$ dominated by lower-band chorus.

away from the magnetic equator. This could be due to the propagation of chorus waves from the generation region in the vicinity of magnetic equator (e.g. LeDocq et al., 1998; Parrot et al., 2003) assuming that the chorus waves are generated mainly outside plasmapause while Cluster crosses the equator inside plasmapause.

The shape of spectral density distribution shown in Fig. 3 resembles the distribution of lower-band chorus derived from CRRES measurements for latitudes MLat>15° (see Plate 4 in Meredith et al., 2001, or top row in Fig. 6 of Bortnik et al., 2007), while CRRES distributions of lower-band chorus for MLat<15° (see Plate 3 in Meredith et al., 2001, or bottom row in Fig. 6 of Bortnik et al., 2007) looks substantially different. The fact that Cluster results resemble CRRES distributions of chorus at higher latitudes but differ from CRRES distributions near the equator is likely to be due to the difference between Cluster high-inclination orbit and CRRES orbit with inclination of 18°, i.e. Cluster goes too deep into the plasmasphere near its perigee to detect the intense nightside chorus near the equator.

Distribution of spectral density in the frequency range dominated by upper-band chorus ($0.5 \leq f/f_{ce} < 1$) is shown in Fig. 4. Unfortunately, the frequency range of Cluster STAFF spectrum analyzer allows to scan frequencies above 0.5 f_{ce} only at low L-shells. Thus the spectral distribution in Fig. 4 only covers upper-band chorus waves occurring within $L \sim 5.5$. The distribution shows the maximum intensity of upper-band chorus in post-midnight and morning MLT sectors which is consistent with Meredith et al. (2001) who reported the maximum intensity of upper-band chorus in the morning sector.

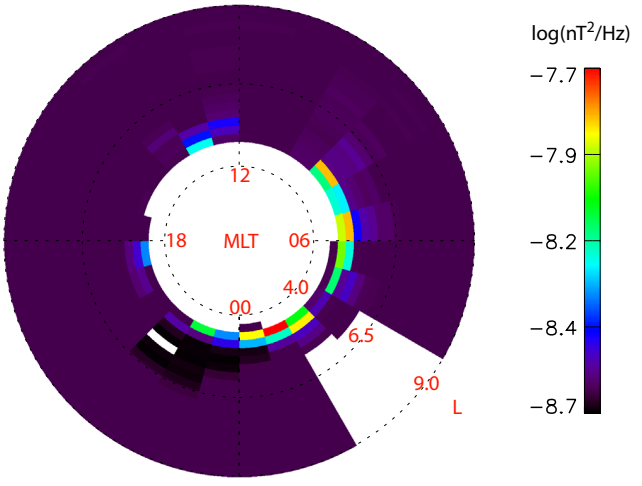

Fig. 4. Distribution of the spectral density in the frequency range $0.5 \leq f/f_{ce} < 1$ dominated by upper-band chorus.

4.5 Dependence on global magnetospheric activity

Since few models of radiation belt dynamics (e.g. Bourdarie et al., 1996; Shprits and Thorne, 2004) utilize three-hour K_p index as an indicator of global disturbance in this study we use the K_p index to illustrate the dependance of wave intensity on the global magnetospheric activity, even though other indices could be more relevant to the generation of particular types of plasma waves. Cluster STAFF-SA dataset have been separated into three groups representing high ($K_p \geq 5o$), moderate ($3o \leq K_p < 5o$) and low ($K_p < 3o$) levels of geomagnetic activity.

Dependance of magnetosonic waves ($0.0005 \leq f/f_{ce} < 0.02$), plasmaspheric hiss

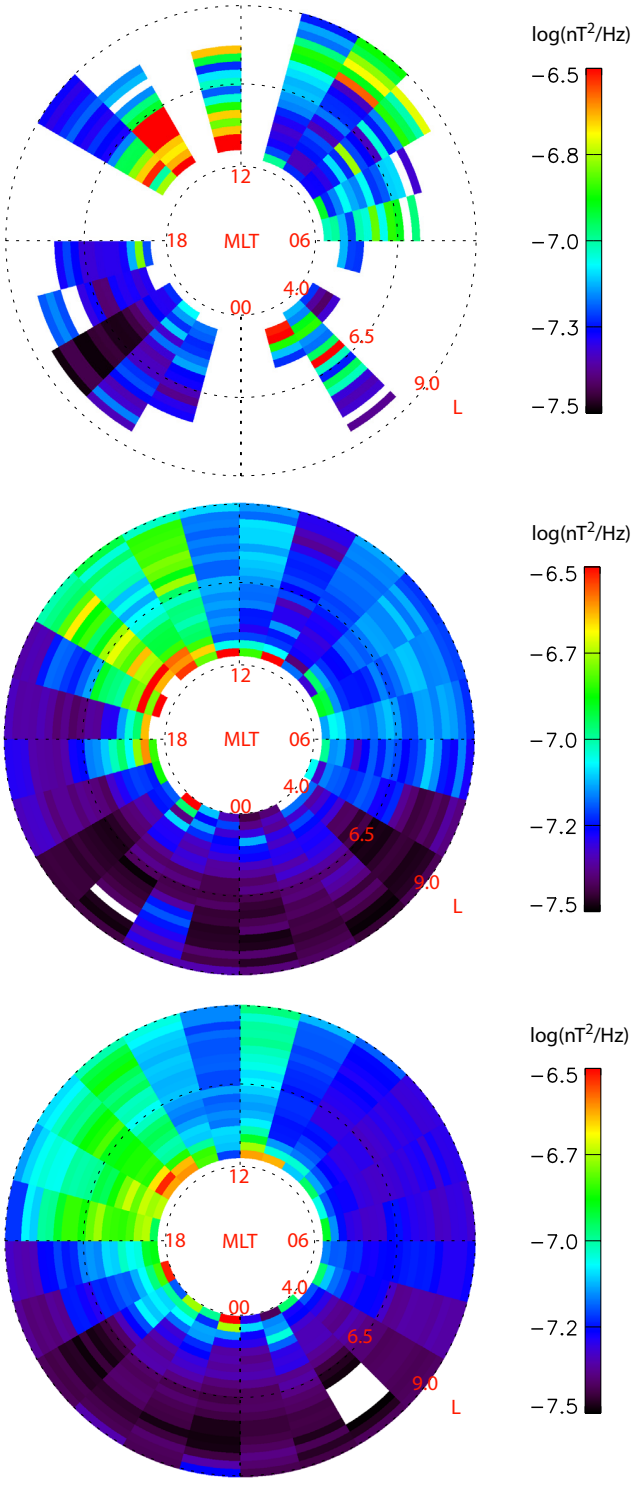

Fig. 5. Distributions of the spectral density in the frequency range $0.0005 \leq f/f_{ce} < 0.02$ (magnetosonic waves) for different K_p levels. Top, central, and bottom panel corresponds, respectively, to high ($K_p \geq 5o$), moderate ($3o \leq K_p < 5o$), and low ($K_p < 3o$) levels of magnetospheric activity.

($0.02 \leq f/f_{ce} < 0.1$) and lower-band chorus ($0.1 \leq f/f_{ce} < 0.5$) on global magnetospheric disturbance level is illustrated, respectively, in Figs. 5, 6 and 7. Obviously, the periods of high magnetospheric disturbance have relatively poor data coverage (see top panels in Figs. 5–7).

Lower-band chorus waves in Fig. 7 demonstrate very strong dependance on the magnetospheric activity with the maximum intensity of chorus waves apparently shifting from post-noon to pre-noon/morning MLT sectors as the activity level goes up. It has been suggested that high latitude chorus on the dayside could be generated above the magnetic equator in the minimum magnetic field pockets produced by the solar wind compression of the magnetosphere (Tsurutani and Smith, 1977). Since chorus wave power becomes more restricted to lower L with increasing magnetic activity in Fig. 7, this could be due to a more compressed magnetopause during active conditions which restricts wave generation to lower L. Ray tracing in a compressed magnetic field needs to be considered to verify this idea.

Plasmaspheric hiss also shows strong dependence on global activity as shown in Fig. 6. While for low K_p (bottom panel in Fig. 6) hiss shows relatively uniform distribution over 08:0–18:00 MLT sector, for moderate K_p levels (central panel) hiss distribution has clear peak in 13:00–17:00 MLT sector. Similar behavior of plasmaspheric hiss has been observed in CRRES data (see Fig. 3 in Meredith et al. (2004)). Apparent reduction of hiss intensity during highly-disturbed periods ($K_p \geq 5o$) seen in the top panel of Fig. 6 is probably due to the fact that during these disturbed periods the plasmasphere gets eroded and thus Cluster perigee lies outside the region dominated by plasmaspheric hiss.

In contrast to hiss and chorus, the intensity of magnetosonic waves in Fig. 5 shows relatively weak dependance on K_p level, with the peak intensity in post-noon MLT sector. While Kasahara et al. (1994) also reported weak or no dependence on geomagnetic activity for the magnetosonic waves, André et al. (2002) suggested that the "equatorial noise" was mainly observed during periods of strong magnetic activity. It has to be noted that the definition of "equatorial noise" adopted by André et al. (2002) includes not only magnetosonic waves occurring above local f_{cH} but also ion-cyclotron waves below f_{cH}, while Cluster STAFF-SA data only includes the waves above f_{cH}.

5 Conclusions

A four year long dataset of Cluster STAFF-SA experiment has been processed to create the statistical distributions of wave spectral density in the ELF-VLF frequency range between local f_{cH} and local f_{ce}. The resulting statistical distributions cover four essential frequency ranges: $0.0005 \leq f/f_{ce} < 0.02$ dominated by equatorial magnetosonic waves, $0.02 \leq f/f_{ce} < 0.1$ dominated by plasmaspheric hiss, $0.1 \leq f/f_{ce} < 0.5$ dominated by lower-band

chorus and $0.5 \leq f/f_{ce} < 1$ range dominated by upper-band chorus waves. The use of normalized frequencies for the database construction helps to discriminate chorus waves from plasmaspheric hiss though at high latitudes some ambiguity still remains due to the fact that plasmaspheric hiss appear at wide range of frequencies and not related to the local gyrofrequency. This ambiguity can be resolved either through physical considerations described in Sect. 4.3, or in a more regular way, by performing the coherency analysis of Cluster dataset.

Analysis of statistical distributions in the range $0.0005 \leq f/f_{ce} < 0.02$ confirms that the magnetosonic waves are closely confined to the equatorial region within $\pm 5°$ MLat. It also outlines the important fact that the equatorial magnetosonic waves have maximum intensity in the post-noon sector near 14:00–20:00 MLT. Spectral density distributions in the range $0.02 \leq f/f_{ce} < 0.1$ demonstrate that plasmaspheric hiss appearing in the regions near the plasmapause ($L < 6$) dominates local time sectors from 06:00 to 18:00 MLT with maximum magnitudes observed in 13:00–17:00 MLT sector. Distributions of spectral density in the range $0.1 \leq f/f_{ce} < 0.5$ show the presence of chorus waves in MLT sectors from 05:00 to 18:00 MLT with a maximum intensity in post-noon sector. Lower-band chorus distributions appear to be consistent with the distribution of chorus observed by CRRES spacecraft at latitudes above 15° MLat (Meredith et al., 2001). Distribution of spectral density in the range $0.5 \leq f/f_{ce} < 1$ (only partially covered by the STAFF spectrum analyzer) shows that the upper-band chorus waves have maximum intensity in post-midnight and morning MLT sectors. Chorus and plasmaspheric hiss show strong dependance on geomagnetic activity while equatorial magnetosonic emissions demonstrate weaker dependence on K_p level.

It has been demonstrated that Cluster STAFF-SA experiment is capable of extracting some features of the distributions of magnetosonic waves, plasmaspheric hiss and chorus that have not been analyzed before (such as MLT distributions of magnetosonic waves and distribution of chorus at high latitudes). Spacecraft datasets used to construct the existing wave models have considerable limitations. For instance, due to its orbit configuration the DE-1 spacecraft (André et al., 2002) provides limited coverage of the radiation belt regions outside $L \sim 5$ and has coverage gaps in the evening MLT sector. CRRES dataset (Meredith et al., 2001, 2004) only covers the regions inside MLat $< 30°$ and has relatively poor statistical coverage in pre-noon MLT sector. Also, CRRES instrument is only able to detect waves below lower-hybrid frequency at lower L-shells and thus is not very suitable for the statistical analysis of equatorial magnetosonic waves. In contrast, Cluster dataset of four years has nearly uniform coverage in MLT thus providing good statistics in the region around the equatorial plasmapause which is important for the generation of chorus and magnetosonic waves. Cluster also extends the coverage to higher latitudes

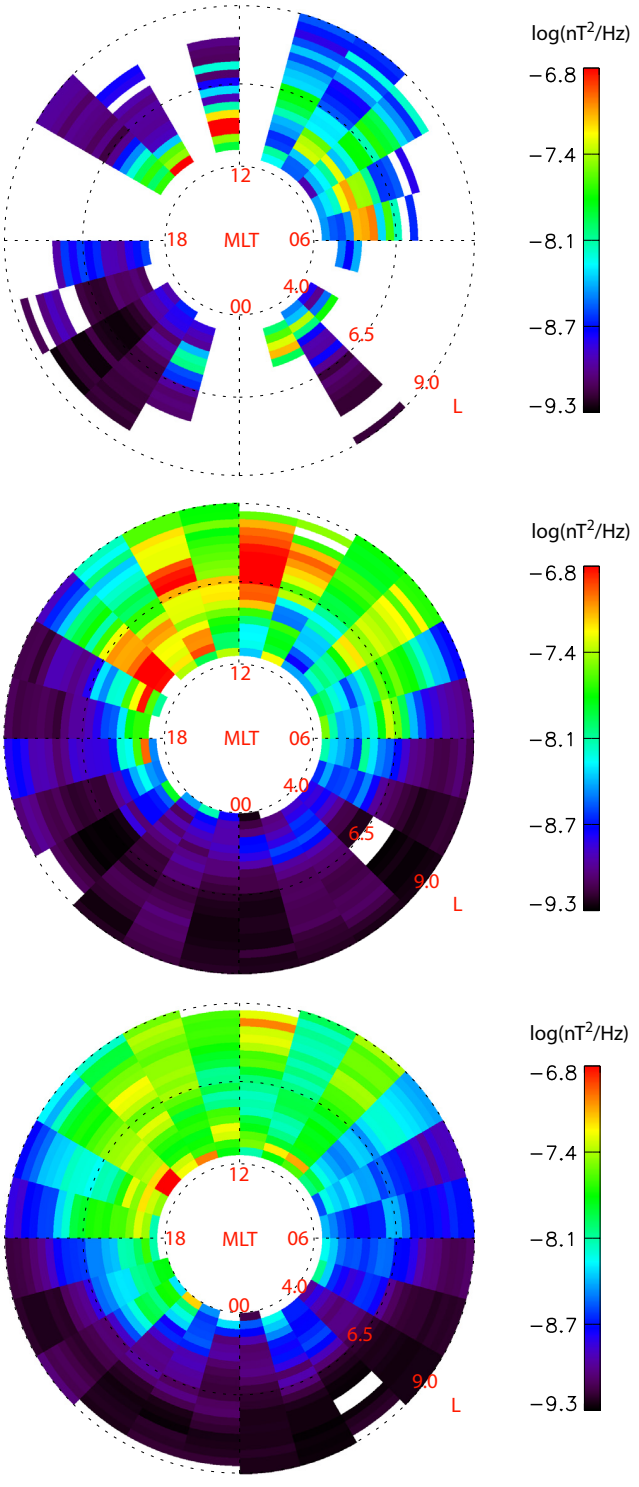

Fig. 6. Distributions of the spectral density in the frequency range $0.02 \leq f/f_{ce} < 0.1$ (plasmaspheric hiss) for different K_p levels. Top, central, and bottom panel corresponds, respectively, to high ($K_p \geq 5o$), moderate ($3o \leq K_p < 5o$), and low ($K_p < 3o$) levels of magnetospheric activity.

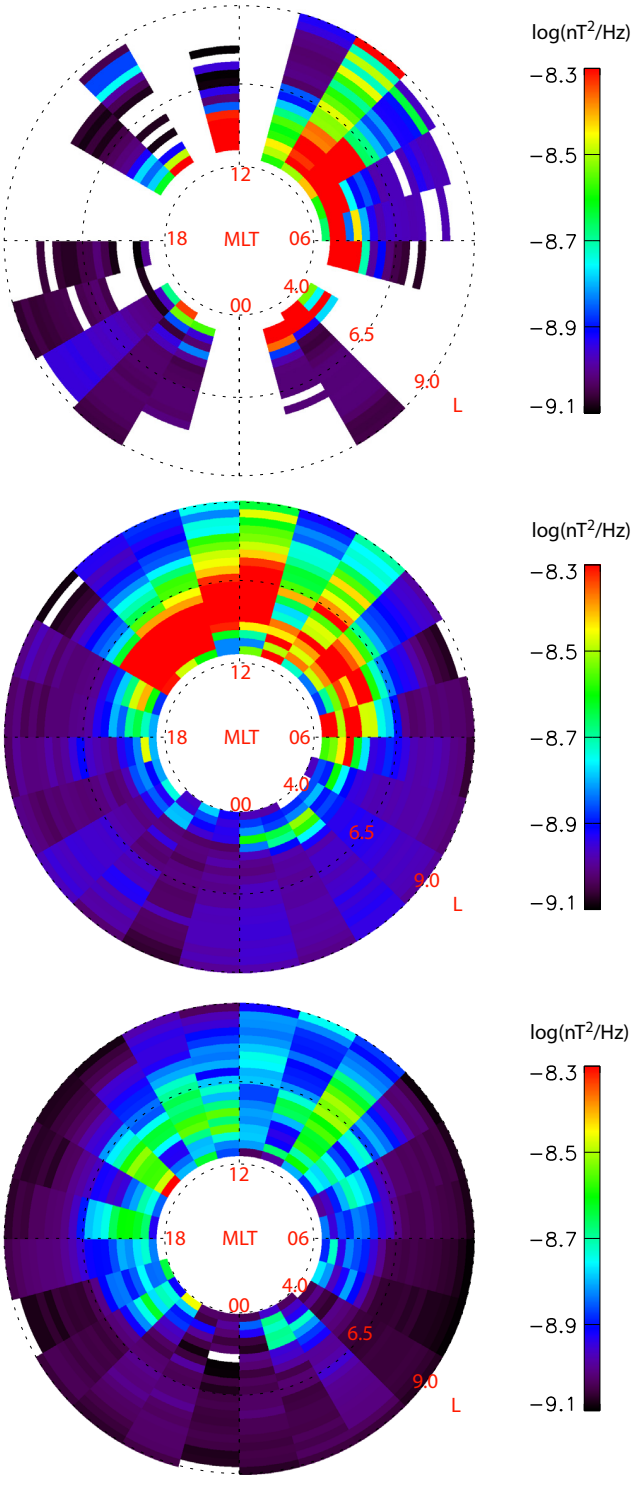

Fig. 7. Distributions of the spectral density in the frequency range $0.1 \leq f/f_{ce} < 0.5$ (lower-band chorus) for different K_p levels. Top, central, and bottom panel corresponds, respectively, to high ($K_p \geq 5o$), moderate ($3o \leq K_p < 5o$), and low ($K_p < 3o$) levels of magnetospheric activity.

not covered by CRRES and DE-1 thus providing the information needed to calculate bounce averaged diffusion rates (Glauert and Horne, 2005). On the negative site, Cluster dataset covers narrow range of L-shells at a given latitude (e.g. Cluster always crosses the equatorial plane at $L \sim 4.5$). Taking into account all the limitations it would be beneficial to combine the existing databases into unified multi-spacecraft database that would become an operational tool for radiation belt modeling.

Acknowledgements. We are grateful to D. Boscher and S. Bourdarie of ONERA/DESP and to N. P. Meredith of British Antarctic Survey for valuable discussions of various aspects of wave-particle interactions and radiation belt modeling. We are also grateful to the ESA Cluster Active Archive team for making available the dataset of Cluster STAFF-SA experiment. We would like to acknowledge financial support from the UK STFC and from the International Space Science Institute in Bern, Switzerland within the framework of the ISSI Team 89: "On the use of wave field measurements to trace WPI in the plasmasphere and at medium and low latitude ionosphere".

Topical Editor I. A. Daglis thanks two anonymous referees for their help in evaluating this paper.

References

Abel, B. and Thorne, R. M.: Electron scattering loss in Earth's inner magnetosphere – 1. Dominant physical processes, J. Geophys. Res., 103, 2385–2396, 1998.

André, R., Lefeuvre, F., Simonet, F., and Inan, U. S.: A first approach to model the low-frequency wave activity in the plasmasphere, Ann. Geophys., 20, 981–996, 2002, http://www.ann-geophys.net/20/981/2002/.

Bortnik, J., Thorne, R. M., and Meredith, N. P.: Modeling the propagation characteristics of chorus using CRRES suprathermal electron fluxes, J. Geophys. Res., 112, A08204, doi:10.1029/2006JA012237, 2007.

Bourdarie, S., Boscher, D., Beutier, T., Sauvaud, J. A., and Blanc, M.: Magnetic storm modeling in the earth's electron belt by the Salammbô code, J. Geophys. Res., 101, 27 171–27 176, 1996.

Cornilleau-Wehrlin, N., Gendrin, R., Lefeuvre, F., Parrot, M., Grard, R., Jones, D., Bahnsen, A., Ungstrup, E., and Gibbons, W.: VLF electromagnetic waves observed on-board GEOS-1, Space Sci. Rev., 22, 371–382, 1978.

Cornilleau-Wehrlin, N., Chauveau, P., Louis, S., Meyer, A., Nappa, J. M., Perraut, S., Rezeau, L., Robert, P., Roux, A., de Villedary, C., de Conchy, Y., Friel, l., Harvey, C. C., Hubert, D., Lacombe, C., Manning, R., Wouters, F., Lefeuvre, F., Parrot, M., Pinçon, J.-L., Poirier, B., Kofman, W., and Louarn, Ph.: The CLUSTER Spatio-Temporal Analysis of Field Fluctuations (STAFF) Experiment, Space Sci. Rev., 79, 107–136, 1997.

Cornilleau-Wehrlin, N., Chanteur, G., Perraut, S., Rezeau, L., Robert, P., Roux, A., de Villedary, C., Canu, P., Maksimovic, M., de Conchy, Y., Hubert, D., Lacombe, C., Lefeuvre, F., Parrot, M., Pinçon, J.-L., Décréau, P. M. E., Harvey, C. C., Louarn, Ph., Santolik, O., Alleyne, H. St. C., Roth, M., Chust, T., Le Contel, O., and STAFF team: First results obtained by the Clus-

ter STAFF experiment, Ann. Geophys., 21, 437–456, 2003, http://www.ann-geophys.net/21/437/2003/.

Davis, L. R. and Williamson, J. M.: Low-energy trapped protons, Space Res., 3, 365–375, 1963.

Glauert, S. A. and Horne, R. B.: Calculation of pitch angle and energy diffusion coefficients with the PADIE code, J. Geophys. Res., 110, A04206, doi:10.1029/2004JA010851, 2005.

Green, J. L., Boardsen, S., Garcia, L., Taylor, W. W. L., Fung, S. F., and Reinisch, B. W.: On the origin of whistler mode radiation in the plasmasphere, J. Geophys. Res., 110, A03201, doi:10.1029/2004JA010495, 2005.

Gustafsson, G., André, M., Carozzi, T., Eriksson, A. I., Fälthammar, C.-G., Grard, R., Holmgren, G., Holtet, J. A., Ivchenko, N., Karlsson, T., Khotyaintsev, Y., Klimov, S., Laakso, H., Lindqvist, P.-A., Lybekk, B., Marklund, G., Mozer, F., Mursula, K., Pedersen, A., Popielawska, B., Savin, S., Stasiewicz, K., Tanskanen, P., Vaivads, A., and Wahlund, J.-E.: First results of electric field and density observations by Cluster EFW based on initial months of operation, Ann. Geophys., 19, 1219–1240, 2001, http://www.ann-geophys.net/19/1219/2001/.

Hapgood, M. A., Dimbylow, T. G., Sutcliffe, D. C., Chaizy, P. A., Ferron, P. S., Hill, P. M., and Tiratay, X. Y.: The Joint Science Operation Centre, Space Sci. Rev., 79, 487–525, 1997.

Horne, R. B. and Thorne, R. M.: Potential waves for relativistic electron scattering and stochastic acceleration during magnetic storms, Geophys. Res. Lett., 25, 3011–3014, 1998.

Horne, R. B., Thorne, R. M., Shprits, Y. Y., Meredith, N. P., Glauert, S. A., Smith, A. J., Kanekal, S. G., Baker, D. N., Engebretson, M. J., Posch, J. L., Spasojevic, M., Inan, U. S., Pickett, J. S., and Decreau, P. M. E.: Wave acceleration of electrons in the Van Allen radiation belts, Nature, 437, 227–230, 2005.

Horne, R. B., Thorne, R. M., Glauert, S. A., Meredith, N. P., Pokhotelov, D., and Santolík, O.: Electron acceleration in the Van Allen radiation belts by fast magnetosonic waves, Geophys. Res. Lett., 34, L17107, doi:10.1029/2007GL030267, 2007.

Kasahara, Y., Kenmochi, H., and Kimura, I.: Propagation characteristics of the ELF emissions observed by the satellite Akebono in the magnetic equatorial region, Radio Sci., 4, 751–768, 1994.

Lyons, L. R. and Thorne, R. M.: Equilibrium structure of radiation belt electrons, J. Geophys. Res., 78, 2142–2149, 1973.

LeDocq, M. J., Gurnett, D. A., and Hospodarsky, G. B.: Chorus source locations from VLF Poynting flux measurements with the polar spacecraft, Geophys. Res. Lett., 25, 4063–4066, 1998.

Lefeuvre, F. and Parrot, M.: The use of the coherence function for the automatic recognition of chorus and hiss observed by GEOS, J. Atmos. Terr. Phys., 41, 143–152, 1979.

Meredith, N. P., Horne, R. B., and Anderson, R. R.: Substorm dependence of chorus amplitudes: Implications for the acceleration of electrons to relativistic energies, J. Geophys. Res., 106, 13 165–13 178, 2001.

Meredith, N. P., Horne, R. B., Thorne, R. M., Summers, D., and Anderson, R. R.: Substorm dependence of plasmaspheric hiss, J. Geophys. Res., 109, A06209, doi:10.1029/2004JA010387, 2004.

Meredith, N. P., Horne, R. B., Clilverd, M. A., Horsfall, D., Thorne, R. M., and Anderson, R. R.: Origins of plasmaspheric hiss, J. Geophys. Res., 111, A09217, doi:10.1029/2006JA011707, 2006.

Parrot, M. and Lefeuvre, F.: Statistical study of the propagation characteristics of ELF hiss observed on GEOS-1, inside and outside the plasmasphere, Ann. Geophys., 4, 363–384, 1986, http://www.ann-geophys.net/4/363/1986/.

Parrot, M., Santolík, O., Cornilleau-Wehrlin, N., Maksimovic, M., and Harvey, C. C.: Source location of chorus emissions observed by CLUSTER, Ann. Geophys., 21, 473–480, 2003, http://www.ann-geophys.net/21/473/2003/.

Perraut, S., Roux, A., Robert, P., Gendrin, R., Sauvaud, J.-A., Bosqued, J.-M., Kremser, G., and Korth, A.: A systematic study of ULF waves above f_{H^+} from GEOS 1 and 2 measurements and their relationship with proton ring distributions, J. Geophys. Res., 87, 6219–6236, 1982.

Russell, C., Holzer, R., and Smith, E.: OGO 3 observations of ELF noise in the magnetosphere : 1. spatial extent and frequency of occurrence, J. Geophys. Res., 74, 755–777, 1969.

Russell, C., Holzer, R., and Smith, E.: OGO 3 observations of ELF noise in the magnetosphere, 2. the nature of the equatorial noise, J. Geophys. Res., 75, 755–768, 1970.

Russell, C., McPherron, R., and Coleman, P.: Fluctuating magnetic fields in the magnetosphere, I: ELF and VLF fluctuations, Space Sci. Rev., 12, 810–856, 1972.

Santolík, O. and Parrot, M.: Application of wave distribution function methods to an ELF hiss event at high latitudes, J. Geophys. Res., 105, 18 885–18 894, 2000.

Santolík, O., Němec, F., Gereová, K., Macúšová, E., de Conchy, Y., and Cornilleau-Wehrlin, N.: Systematic analysis of equatorial noise below the lower hybrid frequency, Ann. Geophys., 22, 2587–2595, 2004, http://www.ann-geophys.net/22/2587/2004/.

Sazhin, S. S. and Hayakawa, M.: Magnetospheric chorus emissions: A review, Planet. Space Sci., 40, 681–697, 1992.

Shprits, Y. Y. and Thorne, R. M.: Time dependent radial diffusion modeling of relativistic electrons with realistic loss rates, Geophys. Res. Lett., 31, L08805, doi:10.1029/2004GL019591, 2004.

Sonwalkar, V. S. and Inan, U. S.: Lightning as an embryonic source of VLF hiss, J. Geophys. Res., 94, 6986–6994, 1989.

Storey, L. R. O., Lefeuvre, F., Parrot, M., Cairó, L., and Anderson, R. R.: Initial survey of the wave distribution function for plasmaspheric hiss observed by ISEE-1, J. Geophys. Res., 96, 19 469–19 489, 1991.

Summers, D., Thorne, R. M., and Xiao, F.: Relativistic theory of wave-particle resonant diffusion with application to electron acceleration in the magnetosphere, J. Geophys. Res., 103, 20 487–20 500, 1998.

Taylor, W. W. L. and Gurnett, D. A.: The morphology of VLF emissions observed with the Injun 3 satellite, J. Geophys. Res., 73, 5615–5626, 1968.

Thorne, R. M., Smith, E. J., Burton, R. K., and Holzer, R. E.: Plasmaspheric hiss, J. Geophys. Res., 78, 1581–1596, 1973.

Tsurutani, B. T. and Smith, E.: Two types of magnetospheric ELF chorus and their substorm dependencies, J. Geophys. Res., 82, 5112–5128, 1977.